Backward can extrusion with conical,rotating punch as a cold forging tribology test

Ceron, Ermanno; Bay, Niels Oluf; Tetsuo, A.; Dohda, K.

Published in:
44th ICFG (International Cold Forging Group) Plenary Meeting

Publication date:
2011

Document Version
Publisher's PDF, also known as Version of record

44th ICFG Plenary Meeting
Proceedings
International Cold Forging Group

Backward Can Extrusion with Conical, Rotating Punch as a Cold Forging Tribology Test

E. Ceron[1]
N. Bay[1]
A. Tetsuo [2]
K. Dohda[3]

[1]Department of Mechanical Engineering, Technical University of Denmark
[2]Graduate School of Science and Engineering for Research, University of Toyama
[3]Department of Mechanical Engineering, Nagoya Institute of Technology

A new, simulative test of friction and lubrication in cold forging is developed by the authors. The test is based on a backward can extrusion process in which the workpiece rotates. An analytical model is presented determining the friction stress from the measured torque during testing combined with an analysis of the sliding velocity distribution along the punch nose. The latter is determined by FE analysis of the test. Results show friction stress for unalloyed low C-steel provided with different types of lubricants, e.g. phosphate coating plus soap, phosphate coating plus MoS_2 and single bathe lubrication with PULS. The new test is so severe, that it is possible to break down the best lubrication systems for cold forging, such as phosphate coating plus soap and MoS_2.

Keywords: Cold Forging, Friction, Limits of Lubrication

Nomenclature

A_0: Initial, local surface area of workpiece
A_1: Final, local surface area of workpiece
B: Geometrical parameter, Eqn. (11)
d_0: Container bore diameter
d_p: Punch diameter, maximum
m_i: Factor in Eqn. (6)
M: Torque
N: Speed of rotation
p: Normal pressure
q_i: Factor in Eqn. (6)
r_a: Minimum radius of punch zone i-th, Fig. 6
r_b: Maximum radius of punch zone i-th, Fig. 6
R: Reduction in can extrusion
T: Temperature of tool surface
v: Relative velocity between punch nose and workpiece material
v_a: Relative velocity component in vertical plane along conical punch nose
v_c: Circumferential component of v
v_p: Punch velocity
v_r: Radial component of v_a
v_v: Vertical component of v_v
z: Relative can height, Eqn. (12)
β: Local slope of conical punch nose
φ: Angle between v_a and v_v
σ_f: Flow stress of deformed material
τ: Friction stress
τ_c: Frictions stress component in circumferential direction

1. Introduction

The tribological conditions in cold forging are varied, depending on the actual process involved (upsetting, ironing, rod extrusion or can extrusion). In testing of friction and limits of lubrication in these processes, great difficulties are encountered due to limitations in variation of tool and process parameters. As regards the tool, it is often expensive or difficult to carry out parametric studies varying material, surface topography, coating and temperature. Concerning the process parameters, normal pressure, surface expansion, sliding length, sliding velocity and tool temperature, it is a problem that these parameters are normally impossible to vary independently of each other. This problem implies the necessity of adopting simulative tests, which should preferably model the tribological conditions in a controlled way, i.e. with controlled and measurable process parameters reflecting the real process conditions in a satisfactory way.

As regards modeling of cold forging and cold extrusion operations it is important to assure gross plastic deformation A_1/A_0 = 1-50 under well controlled normal pressures p in a wide range p/σ_f = 0-5. Tool temperatures are also of importance to control in cold forging varying in the range T = 20-200°C or more (spike temperatures may reach values of 600°C in can extrusion of steel). The broad range of the process parameters A_1/A_0 and p/σ_f is difficult to control in a single type of test and Bay et al. [1-2] have proposed to apply a system of tests instead. Fig. 1 shows a schematic outline of these tests. Fig. 1a is the compression-twist test of a circular cylindrical specimen between plane overhanging anvils. The test may be carried out with initial compression followed by twisting under constant load or with simultaneous compression and twisting. The normal pressure range is 0-≈1 times the flow stress of the deformed material, see Table 1.

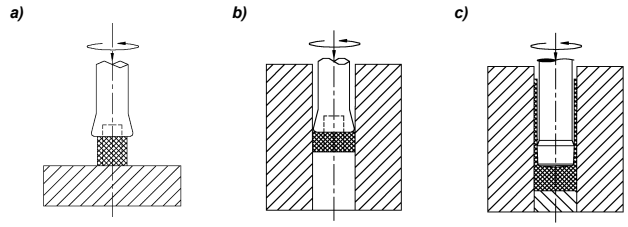

Figure 1. Schematic outline of developed system of tests, a) compression-twist test, b) compression-twist test in closed die, c) backward can extrusion with simultaneous punch rotation.

Fig. 1b shows a compression-twist test performed in a closed die, allowing for an increase in normal pressure to about 3 times the flow stress of the deformed work piece material in case of steel (5 times in case of aluminum). In the two tests Fig. 1a and b the surface expansion is varied by varying the initial height and diameter of the billets upsetting to the same final diameter. Fig. 1c shows a backward can extrusion with simultaneous rotation of the punch with respect to the work piece and the die performed under constant load. In this test a large punch land is applied thus measuring the total friction on the land and the end face of the punch. Subtracting the torque measured when testing with a smaller punch land the net friction on the land is determined. In order to ensure a well-defined normal pressure the punch land is slightly conical, with an included angle of 4°. The surface expansion is varied in this test by varying the extruded can height. The normal pressure in the test surface along the punch land is approximately equal to the flow stress of the deformed material, [3].

Table 1
Parameter range for the tests in Fig 1.

	Test		
Parameter	**A**	**B**	**C**
Normal pressure	$0 \le p/\sigma_f \le 1$	$0 \le p/\sigma f \le$ 3-5	$p/\sigma f \approx 1$
Surface expansion, $X=(A_1-A_0)/A_0$	$0 \le X \le 3$	$0 \le X \le 3$	$0 \le X \le 50$
Average tool temperature, T[°C]	$20 \le T \le 200$	$20 \le T \le 200$	$20 \le T \le 200$
Sliding length, s [mm]	$0 \le s \le \infty$	$0 \le s \le \infty$	$0 \le s \le \infty$
Sliding velocity, v [mm/s]	$0 \le v \le 50$	$0 \le v \le 50$	$0 \le v \le 50$

Fig. 2 shows a schematic outline of the test equipment designed for a 1500 kN hydraulic press with a max ram speed of 40 mm/sec. The punch is mounted on a combined force and torque transducer 2 designed as a strain gauge equipped, spoked wheel, which is placed on the moving traverse. The lower tool part is possible to rotate with a hydraulic motor 3 combined to the tool via a gear 4 mounted on the periphery of a plate 5 supporting the container 6. The axial roller bearing 7 is able to take up the maximum load of 1500 kN. Radial roller bearings 8 ensure proper lining of the tool. Apart from the workpiece, which is not shown, rotating parts are the container 6, the counter punch 9 the guiding tool 10 and the bottom tool 11. Referring to [2] tests a and b in Fig. 1 have proven valuable to determine friction in cold forging at varying normal pressure and tool temperature as well as surface expansion, the latter in a moderate range, see Table 1. In order to determine friction at high surface expansion and to estimate the limits of lubrication the test in Fig. 1c should be applied.

A disadvantage in the present design of the backward can extrusion test with a rotating punch is the rather small normal pressure on the punch land $p/\sigma_f \approx 1$ and the fact that two tests are required with a large and a small punch land respectively in order to eliminate the friction contribution from the tip of the punch. In the present investigation a new punch design is tested, where these disadvantages are avoided.

The objectives of the present research are to develop a direct tribology test method for cold forging:

- Measuring friction stress at high surface expansion and normal pressure and varying tool temperature
- Testing the limits of lubrication of different lubricants at varying tool temperature

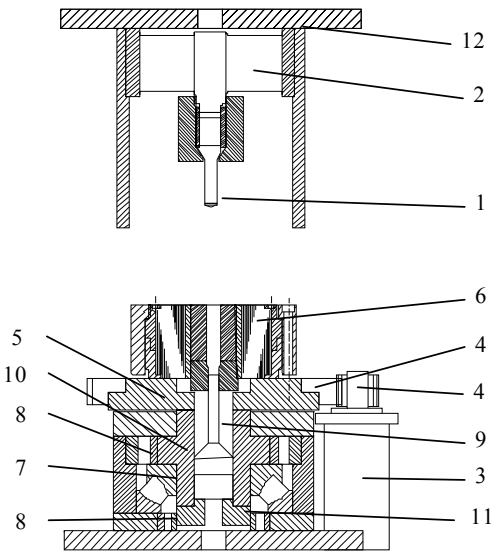

Figure 2. Schematic outline of tribology test equipment.

2. New punch design

Fig. 3a shows the old punch design, whereas Fig. 3b shows the new one. Both punches have a maximum diameter d_p = 15.6 mm which applied together with a container of bore diameter d_0 = 22.0 mm leads to a reduction:

$$R = \frac{d_p^2}{d_0^2} = 0.5 \text{ [MPa]} \qquad (1)$$

The new punch design, produced in three different versions has an almost flat, but slightly conical punch tip with an included angle $2\alpha = 170°$ of rather small diameter, ø5 mm implying that the major part of the punch nose is the conical part with an included angle 2θ = 2x25°, 2x35°, 2x45° respectively.

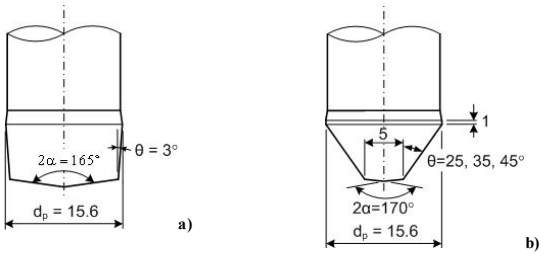

Figure 3. Schematic punch design. a) old, b) new.

With the new design the major contribution to the torque comes from the conical part, where surface expansion as well as normal pressure is rather high.

3. Analysis of material flow and resulting torque

The torque acting from the rotating workpiece in contact with the punch surface is calculated as:

$$\vec{M} = \vec{\tau}_C \times B \text{ [Nm]} \qquad (2)$$

where $\vec{\tau}_C$ is the friction stress along the circumferential direction and B is a geometry factor.

Since the test involves two different motions at the same time, namely a linear, vertical movement of the punch with speed $\vec{v}_p$ and a rotation of the specimen, the resulting friction stress vector $\vec{\tau}$ acting on the conical part of the punch nose varies with the location (varying radius). $\vec{\tau}$ has the same direction as the resulting, relative speed $\vec{v}$ of the workpiece with respect to the punch surface. The vector $\vec{v}$, see Fig. 4a, may be decomposed into two components, namely the circumferential speed $\vec{v}_c$ and the punch speed component $\vec{v}_a$ lying in a plane containing the axis of the punch and being tangential to the surface of the punch.

Assuming the friction stress τ to be constant in absolute value over the entire punch/workpiece interface and relating the measured torque M directly to the circumferential component τ_c of the friction stress the value of τ can be determined. From Fig. 4a it is seen that:

$$\vec{\tau}_c = \vec{\tau} \times \cos\varphi \text{ [MPa]} \qquad (3)$$

The angle φ between $\vec{\tau}$ and $\vec{\tau}_c$ is calculated by determining the components $\vec{v}_a$ and $\vec{v}_c$ of the relative speed vector $\vec{v}$, see Fig. 4a.

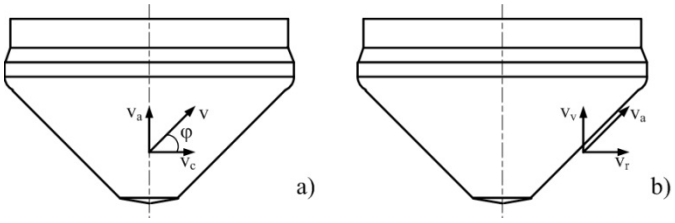

Figure 4. a) Relative speed vector $\vec{v}$ between workpiece and tool, and its two components $\vec{v}_a$ and $\vec{v}_c$; b) speed vector $\vec{v}_a$ and its two components $\vec{v}_v$ and $\vec{v}_r$.

The value of the sliding speed v_a (with respect to the punch) of a point on the workpiece interface, is determined by FE analysis of the backward can extrusion without rotation applying the rigid-plastic code DEFORM™ 2D. The workpiece material was chosen according to the experiments, DIN 1.0303 and a friction factor m = 0.12 was selected as typical for cold forming. The software allows tracking of selected points on the workpiece as they follow the deformation of the material. Regarding the speed, DEFORM™ calculates the absolute values of the vertical v_z and radial v_r components of the tracking point. The vector $\vec{v}_a$ can be split into the two components $\vec{v}_v$ and $\vec{v}_r$ along the directions z and r, as shown in Fig. 5. Since the punch has an absolute speed value $v_p \neq 0$, and v_a is calculated with respect to a reference system which moves with the punch, the relative speed vector $\vec{v}_v$ along the direction of $\vec{v}_z$ is:

$$\vec{v}_v = \vec{v}_z - \vec{v}_p \text{ [m/s]} \qquad (4)$$

Moreover, as the punch movement in radial direction is zero, the radial speed component v_r has the same value and direction in the absolute and the relative reference system. The value of the speed vector $\vec{v}_a$ is therefore determined as:

$$v_a = \sqrt{v_v^2 + v_r^2} = \sqrt{(v_z - v_p)^2 + v_r^2} \text{ [m/s]} \qquad (5)$$

It is thus possible to calculate the value of the vector $\vec{v}_a$ along the entire tool/workpiece interface.

In the numerical simulation a single point was tracked with the initial position on the punch tip r = 1 mm from the centre axis, Fig. 6. The punch tip can be divided in three different zones:

1. small conical surface on the tip of the punch with a diameter of 5 mm
2. the main conical surface with the three inclination angles: θ = 25°, 35°, 45°
3. punch land with almost cylindrical surface

From the experimental data acquired through a Labview program it was possible to calculate the average punch speed v_p in each test.

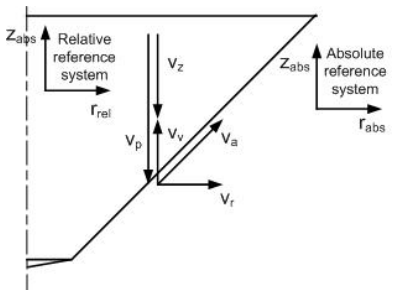

Figure 5. Determination of the resulting sliding speed vector $\vec{v}_a$.

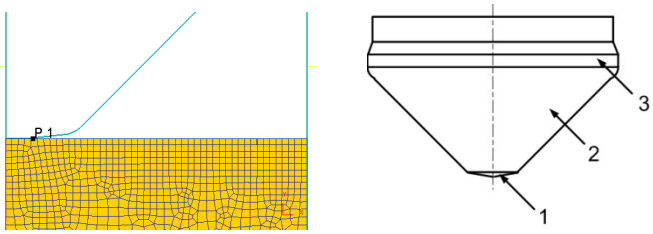

Figure 6. Left: tracked point at the beginning of the simulation. Right: the three conical zones of the punch.

The results showed v_p to be constant throughout the extrusion, for all the punches. Fig. 7 shows the stroke s as a function of the time, during the extrusion, for the three different punch angles θ. The tangent of each curve is the punch speed v_p which as the average value $v_p = 10$ mm/s. This value was inserted in the numerical simulations.

Fig. 8 shows a plot of v_a as a function of the relative radial position $2r/d_p$. The graph is divided into three main regions, corresponding to the three conical parts described above. The region between $0.25 < 2r/d_p < 0.35$ shows an increase of the corresponding to the sudden shift between zone 1 and 2. The region $0.95 < 2r/d_p < 1$ shows the same increase between zone 2 and 3.

As regards the conical regions 1 and 2 of the punch, a linear relationship between v_a and $2r/d_p$ is clearly noticed. The coefficients of the linear equation can easily be determined through a linear regression:

$$v_a = m_i \times \frac{2r}{d_p} + q_i \ \text{[m/s]} \qquad (6)$$

In Table 1 the values of the coefficients m_i and q_i are shown for $v_p = 10$ mm/s, which is approximately the value during testing. In zone 3 the speed v_a is approximately constant due to the small angle and equal to twice value of the punch speed since the reduction is $R = 0.5$. For this case only the q_i coefficients are therefore calculated.

The size of the circumferential speed component $\vec{v}_c$ is given by:

$$v_c = 2\pi r n \ \text{[mm/s]} \qquad (7)$$

where n is the speed of rotation and r is the local radius of the punch where v_c is calculated.

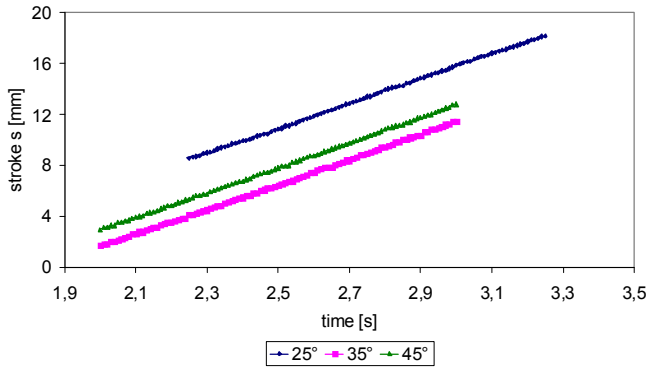

Figure 7. Comparison of the punch speed v_p between the three punches.

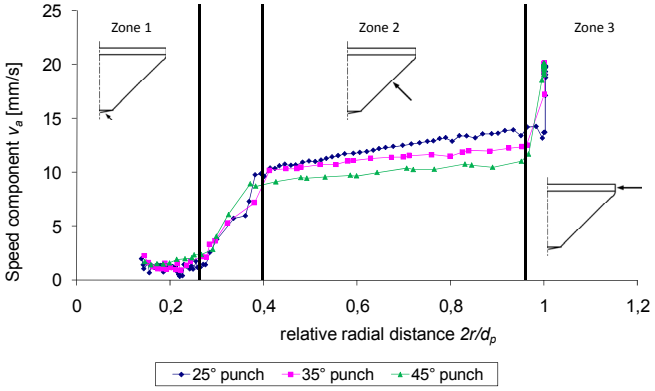

Figure 8. Sliding speed v_a of the track point P1 as a function of the relative radial position, calculated from the numerical simulation for the three different punches geometries.

Table 1.
Coefficients of the linear equation of the speed v_p calculated for a punch speed v_p = 10 mm/s. The subscript refers to the zone on the punch face.

Punch angle θ	m_1 [s^{-1}]	q_1 [mm/s]	m_2 [s^{-1}]	q_2 [mm/s]	q_3 [mm/s]
25°	-0.1565	1.4258	0.8285	7.7816	20
35°	0.3806	0.8726	0.5078	8.6404	20
45°	1.1219	0.0701	0.4989	7.4582	20

Knowing the two speed vectors v_a and v_c, the angle φ determining the local direction of the resulting speed and thus friction stress can be calculated as a function of the radius r:

$$\varphi = \arctan\left(\frac{v_a}{v_c}\right) = \arctan\left[\frac{\sqrt{(v_p - v_z)^2 + v_r^2}}{2\pi \times n \times r}\right] \qquad (8)$$

In order to solve Eqn. (8) analytically, the linear approximation of the speed v_a is inserted in the numerator:

$$\varphi = \arctan\left(\frac{m_i \dfrac{2r}{d_p} + q_i}{2\pi n r}\right) \qquad (9)$$

where i = 1,2,3 indicates the zone where the angle is calculated. Assuming the vector $\vec{\tau}_c$ acts on an infinitesimal area dA , see Fig. 9, this area is expressed as:

$$dA = 2\pi r ds = 2\pi r dr \sin\beta \tag{10}$$

The total torque M is calculated by integration of the local torque contribution dictated by the value of the local circumferential friction stress $\vec{\tau}_c$:

$$\begin{aligned} M &= \int_{r_a}^{r_b} \tau_c 2\pi r \frac{dr}{\sin\beta} r = \frac{2\pi\tau}{\sin\beta}\int_{r_a}^{r_b} \cos\varphi \times r^2 dr = \\ &= \frac{2\pi\tau}{\sin\beta}\int_{r_a}^{r_b} r^2 \cos\left\{\arctan\left[\frac{\sqrt{\left(v_p - v_z\right)^2 + v_r^2}}{2\pi r}\right]\right\} dr = \\ &= \frac{2\pi\tau}{\sin\beta}\int_{r_a}^{r_b} r^2 \cos\left\{\arctan\left(\frac{m_i \times \frac{2r}{d_p} + q_i}{2\pi r}\right)\right\} dr = \tau \times B \end{aligned} \tag{11}$$

The expression inside the integral is non-linear and can be solved by software as Mathlab. The integral is solved for each of the three zones of the punch and the values are reported in Table 2. In every zone the angle β is constant.

Table 2.
Values of coefficient *B*.

Punch angle θ	B_1 [mm³]	B_2 [mm³]	B_3 [mm³]	$B = B_1 + B_2 + B_3$ [mm³]
25°	31	1540.8	299.2	1840
35°	30.1	1181.6	306	1487.6
45°	28.7	1026.2	312.9	1339.1

4. Experiments

Tests on backward can extrusion with rotation were carried out with 3 different punch angles: θ = 25°, 35°, 45°. These three punches were made of CPM® REX 76 PM tool steel and polished with 9µm diamond paste. The workpiece material was low C-steel 1.0303 provided with four lubrication systems:

A. zinc phosphate coating and alkaline soap
B. zinc phosphate coating and MoS_2
C. single bath lubrication system, named PULS, [4-5]

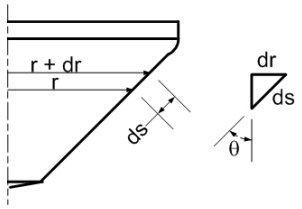

Figure 9. Representation of infinitesimal area where friction stress is calculated.

The slugs have the following sizes: ø22x41 mm. Testing was carried out at two different punch temperatures, i.e. room temperature and 200°C. Heating of the punch tip was done by mounting a copper sleeve fitting the punch tip and provide it with a circumferential electric tube formed electric heater. The copper sleeves for the different punches were manufactured by cold forming in the same container with the same set of punches used for the experiments. They were inserted in a larger copper sleeve made by machining in order to fit in the electric heater. Preheating was done to 220°C, the extra 20°C leaving enough time for preparation of each experiment at a punch temperature of 200°C when starting the test. The temperature was checked by digital thermometer, touching the tip of the punch.

The speed of rotation was n = 20 rpm in each test. It was checked, that n was constant during the test. Testing was done recording the torque as a function of the stroke and plotting the torque as well as the determined friction stress τ as functions of the relative can height $z = h_c / d_p$, using the relation between stroke s and can height h_c based on volume constancy requirements:

$$z = \frac{h_c}{d_p} = \frac{s d_0^2}{d_p\left(d_0^2 - d_p^2\right)} \tag{12}$$

A final relative can height z = 2 was planned.

5. Results

Fig. 10a shows slight pick-up on the conical surface and punch land of the 25° punch when testing lubricant A. In Fig. 10b severe pick-up is formed on the 45° punch testing lubricant C, whereas Fig. 10c shows very severe pick-up on the 35° punch testing aluminium with a poor lubricant. In all cases the pick-up evolution follows a helical pattern corresponding to the local sliding direction on the conical punch nose.

As seen in Fig. 11, the force and torque curves fluctuates, though the fluctuations in the force signal are almost imperceptible. The frequency is appr. 6 Hz. The amplitude seems to increase with the torque and punch speed. The cause is due to the response time of the electronically controlled hydraulic system which provides the rotation of the specimen. Based on the measurements the response time is determined to be t = 0.168 s. Since the torque generated by friction changes during the test, the pump feeding the hydraulic motor is forced to equilibrate it in order to keep a constant speed of rotation. This implies that the oil pressure is continuously adjusted causing a pressure fluctuation which has a frequency of f = 1/t = 1 / 0.168 ≈ 6 Hz.

The torque fluctuation affects the force as well, although the amplitude is much smaller and although the hydraulic system for the extrusion load is completely independent of that for the rotation. Since the yield criterion has to be satisfied in the plastically deforming workpiece material a decrease in friction calls for an increase in normal pressure. It was noticed that a phase shift between force and torque fluctuations was around π thus verifying the cause of the force fluctuations.

In Fig. 12, the friction stress τ is shown for 5 repetition tests with a 25° punch and specimens lubricated with zinc phosphate and soap. The five tests show a good repeatability.

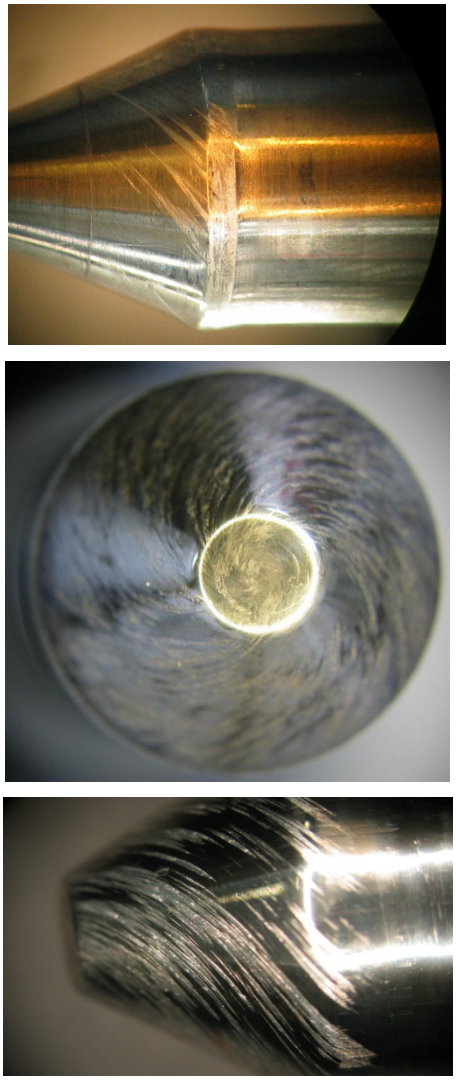

Figure 10. a) side view of 25° punch, slight pick, lubricant A; b) top view of 45° punch, severe pick up, lubricant C; c) side view of 35° punch, very severe pick-up, aluminum with poor lubricant.

In the range $0 \leq z \leq 0.4\text{-}0.7$ the contact surface increases because the workpiece material is sliding on the conical surface of the punch. The analytical model described above is not valid in that range, since it assumes contact in all the three zones described in paragraph 3. Therefore friction stress curves are not shown in this range. After $z \approx 0.5$, τ starts to decrease, likely due to temperature increase but after $z \approx 1.4$ the lubricant film becomes too thin and the friction increases. This behaviour is noticed in every test.

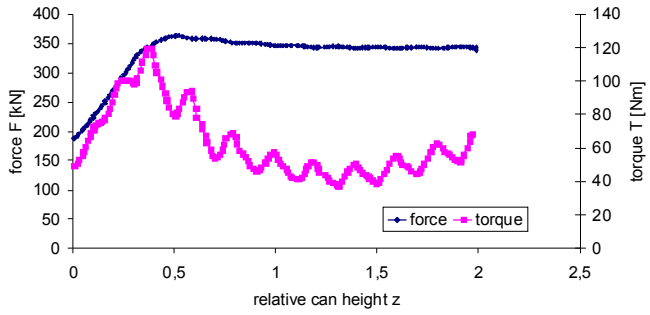

Figure 11. Force and torque results for 25° punch at room temperature.

In Fig. 13, representing lubricant A again, 5 repetitions with 35° punch are shown. In repetitions 2 and 5 slight pick-up occurred. It was, however, not possible to register this slight pick-up on the friction stress curves due to the insignificant change of friction. Fig. 14 showing friction stress for lubricant C using the 35° punch does, however, indicate the observed pick-up due to the fact that it was much more severe. Had the test been performed to a lower, maximum can height, z = 1, pick-up would probably not appear even in this case.

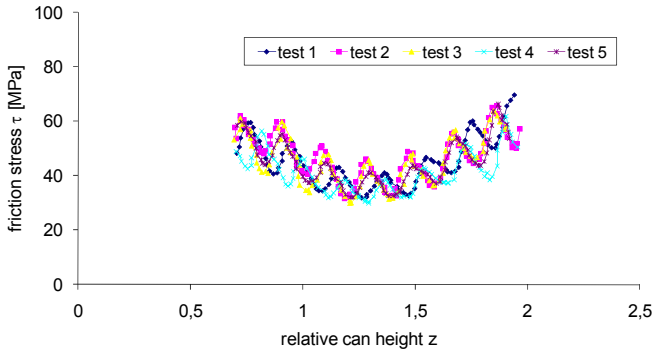

Figure 12. 5 repetition tests for 25° punch, lubricant A.

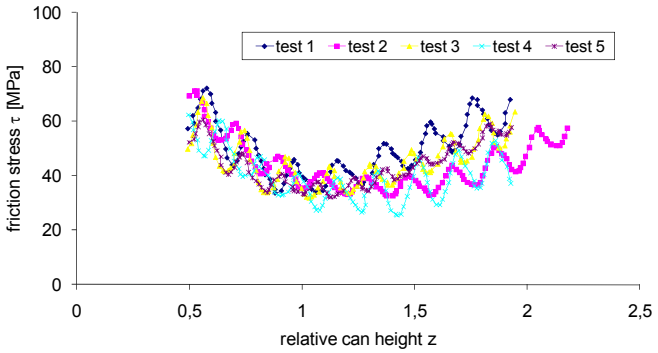

Figure 13. 5 repetition tests for 35° punch, lubricant A.

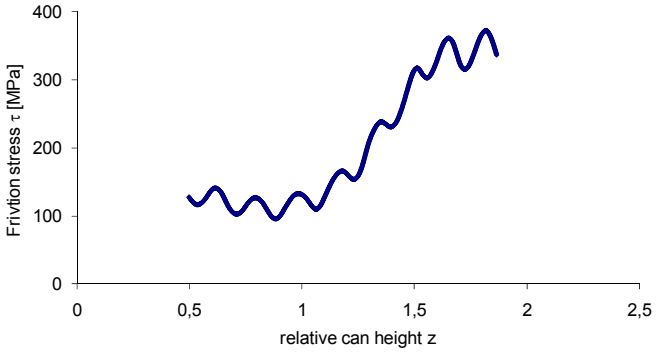

Figure 14. Friction stress τ for 35° punch, lubrication C.

In Fig. 15 a comparison between three tests done with the three different punches is shown. After $z \approx 1$ there is practically no difference between the curves, since the normal pressure at the interface in all cases is high implying that the constant friction model (independent of pressure) applies.

In Table 4 an overview of the performed tests is shown. At first glance, it is realized that the new tribology test is able to breakdown even good lubrication systems such as zinc phosphate and soap. This means that the new test is appropriate for

systematic and quantitative testing limits of lubrication of cold forging tribo-systems. It is noticed that lubricant C fails in all tests. Pick-up and galling were more severe with this lubricant than with lubricants A and B.

As shown in Table 5 the value of the friction stress fluctuates around 40 MPa, for lubrication A, at the lowest point which is around $z \approx 1.2$. For lubrication B, the value increase to 50 MPa. This is in accordance with earlier observations indicating that phosphate coating plus soap gives lower friction than phosphate coating plus MoS_2. Lubricant C resulted in a minimum value of appr. 100 MPa. The reason for this significant increase is probably, that the film thickness is much smaller than for lubricant A and B.

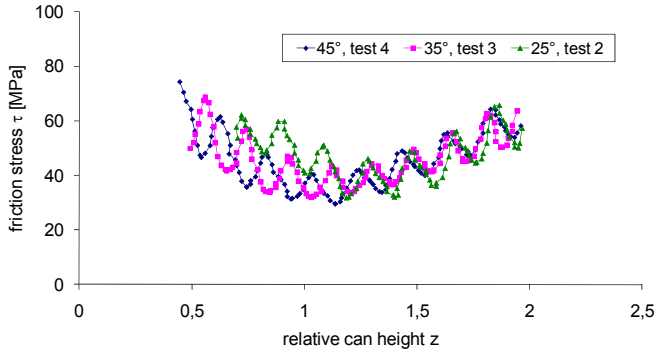

Figure 15. Comparison of friction stress τ between the three different punches.

Table 4.
Performed tests. O = no pick up; P = pick up; X = test not performed.

Temperature [°C]	Punch angle θ	Lubrication A	B	C
20	25°	O	P	P
	35°	P	P	P
	45°	P	O	P
200	25°	O	O	P
	35°	X	P	P
	45°	P	P	P

Table 5.
Friction stress and friction factor m for lubrication A, B and C.

	Lubrication A	B	C
Friction stress τ [MPa]	40	50	100
Friction factor m	0.10	0.13	0.26

6. Conclusions

A new tribology tests for cold forging is presented. The test is based on a backward can extrusion combined with a rotation of the workpiece with respect to the punch. The new punch design ensures high normal pressure and surface expansion, which are essential parameters to investigate the performance of different lubricant systems for cold forging. The conical punch nose increase the severity of the process and allows breakdown of the lubricant film at relative low can height even when using good lubrication such as phosphate coating plus soap or MoS_2. The superimposed rotation of the workpiece with respect to the punch allows measurement of the frictional torque during. A combined numerical and analytical model enables calculation of the friction stress on the punch nose from the measured torque. In this way comparison of different lubricant systems is possible.

Acknowledgements

The authors gratefully acknowledge Mr. Mogens Sørensen at DFT-Presswork A/S, Dr. Søren Lassen at BRDR Jørgensen Components A/S and Dr. Gerhard Linder at Hirschvogel Umformtechnik GmbH for providing the lubrications.

References

[1] Hansen, B., Bay, N., 1986, Two methods for testing lubricants for cold forging, J. Mechanical Working Technology, 13:189-204.

[2] Bay, N. Eriksen, M., Tan, X., Wibom, O., An empirical model for friction in cold forging, Euromech435 colloquium on Simulation of Friction and Wear in Metal Forming, Valenciennes, 18.-20. June 2002, 105-124.

[3] Bay, N., Wibom, O., Nielsen, J., A new friction and lubrication test for cold forging, Annals of CIRP, 44/1/1995.

[4] Yoshida, M., Imai, Y., Yamaguchi, H., Nagata, S., 2003, Nihon Parkerizing, Technical Report No. 15.

[5] Bay, N., Azushima, A., Groche, P., Ishibashi, I., Merklein, M., Morishita, H., Nakamura, T., Schmid, S., Yoshida, M., 2010, Environmentally Benign Tribo-systems for Metal Forming, Annals of CIRP – Manufacturing Technology, 59/2:760-780.